https://doi.org/10.46813/2025-156-043

RADIATION ENHANCED CRYSTALLIZATION OF AMORPHOUS LASER CONDENSATES OF HAFNIA AND ZIRCONIA

A.G. Bagmut
National Technical University "Kharkiv Polytechnic Institute", Kharkiv, Ukraine
E-mail: agbagmut@gmail.com

Amorphous films of hafnia (HfO_2) and zirconia (ZrO_2) were studied for crystallization under the action of an electron irradiation. Electron microscopy studies with "in situ" video recording of structural changes demonstrated, that phase transformation in hafnia is the dendrite polymorphous crystallization mode with the relative length $\delta_0 \approx$ 2380 and in zirconia is the island polymorphous crystallization mode with the relative length $\delta_0 \approx$ 915. The dependence on time of the fraction of the crystalline phase has a quadratic character for hafnia and an exponential one, described by the JMAK formula, for zirconia.

PACS: 61.14.−x, 61.43.Dq, 61.72.Cc, 64.70.Kb, 68.37.Lp, 68.55.A−, 68.37.−d

INTRODUCTION

Hafnia (hafnium dioxide HfO_2) and zirconia (zirconium dioxide ZrO_2) are most attractive for optical coating applications (filters, beamsplitters anti-reflection coatings and high-reflectivity mirrors) and for thin-film electroluminescent (TFEL) applications [1, 2]. Relatively high dielectric constant and large band gap make them one of the most promising materials for the replacement of SiO_2 in the gate oxide insulating layers in metal-oxide-semiconductor (MOS) devices [3]. ZrO_2 and HfO_2 can be grown as a metastable amorphous phase on Si using low-temperature deposition techniques [4].

Hafnia and zirconia films can be deposited by electron beam evaporation, chemical vapor deposition, magnetron sputtering and pulsed laser deposition [1, 5]. Subsequent annealing, which is required at the industrial production stage or natural aging can initiate undesirable crystallization of the amorphous layer. The crystallization of coatings results in a rough microstructure and surface, which significantly affects the optical and electrical properties [3]. Crystallization of amorphous layers depends on the layer thickness: thinner layers have higher crystallization temperatures. So, crystallization temperature of HfO_2 increased from 430 to 600°C when the layer thickness was reduced from 40 to 5 nm [6].

Transition from amorphous to crystalline state is a first-order phase transition (a-c transition). One of its types is polymorphous crystallization, whereby a substance converts from the amorphous into the crystalline state without changes in composition. This is typical for both pure elements and stoichiometric chemical compounds. Spontaneous polymorphous crystallization of amorphous layer (natural aging) can take a long time (years and decades). This complicates the prediction of the reliability and durability of an electronic device. However, there is a possibility of a comprehensive study of the structural transition from amorphous to the crystalline state of matter outside the device. Crystallization modeling can be done inside a transmission electron microscope (TEM).

The passage of electrons through the film causes its Joule-Lenz heating (excitation of phonons) and can creates radiation damage. For excitation of phonons, energy of ~ 0.01 eV is sufficient [7]. Therefore, heating of the film to one degree or another is always present. In a certain mode of operation of the microscope, the electron beam, that forms an image, can initiate the crystallization of an object with amorphous structure. In this case a-c transition can be observed visually ("in situ" method). The combination of different TEM operating modes provides comprehensive information on the structural, morphological, and kinetic parameters of the crystallization process.

The monoclinic modification of hafnia is stable up to 2196°C. Its structural data are: a = 0.51157 nm, b = 0.51819 nm, c = 0.52851 nm, and β = 99.259° [8]. At above 2196°C this modification transforms into the tetragonal modification with parameters a = 0.514 nm and c = 0.525 nm [9]. The orthorhombic modification of HfO_2 has the following parameters: a = 0.5008 nm, b = 0.5062 nm, c = 0.5223 nm [10].

Zirconia also has various polymorphic modifications. Monoclinic modification exists below 1170°C [11]: a = 0.53129 nm, b = 0.52125 nm, c = 0.51471 nm, and β = 99.218°. Above 1170 °C, this modification transforms to the tetragonal one with parameters a = 0.512 nm and c = 0.525 nm [12]. At T ≥ 2370 °C the polymorphous transformation of the tetragonal phase to the cubic one, for which a = 0.509 nm and a space group Fm3m, takes place [13].

In most cases, the kinetics of the a-c process is adequately described with the classic Johnson-Mehl-Avrami-Kolmogorov (JMAK) theory through the equation:

$$x(t) = 1\text{-}\exp(-kt^n), \quad (1)$$

where x is the a-c transformed volume fraction; t is time; k is a rate constant, and n is the Avrami exponent, which is sensitive to the time-dependence of nucleation and to the dimensionality of growth [14–16]. *In situ* studies have shown, that in the case of exponential dependence (1) polycrystalline films are formed. In this case island polymorphous crystallization (IPC) mode takes place [17]. In the case of layer polymorphous crystallization (LPC) mode and dendrite polymorphous crystallization (DPC) mode the quadratic dependence $x(t)$ is fulfilled [18].

Each substance reveals its own path of transition from an amorphous state to a crystalline one. The

classification of these pathways, carried out according to the most appropriate parameters, provides both qualitative and quantitative systematization of the phase transformation. As applied to thin amorphous films, that crystallize under the influence of electron irradiation, the appropriate parameters are structural and morphological characteristics. These are the size, shape, structure, orientation, and number density of crystalline nuclei, growing in an amorphous medium. The relative length δ_0, considered in this work, can serve as a quantitative characteristic of the crystallization mode. This is a dimensionless number, equal to the ratio of the characteristic unit of length to the value of the geometric parameter of the elementary cell of the crystal.

Quantification of the crystallization mode (LPC, DPC ore IPC) can be done on the basis of the value of relative length δ_0, defined as

$$\delta_0 = \frac{D_0}{a_0} \tag{2}$$

in the case of LPC, and as

$$\delta_0 = \frac{D_0}{\sqrt[3]{\Omega}} \tag{3}$$

in the case of IPC and DPC.

Characteristic unit length D_0 is the crystal size at time t_0, after which the volume of the amorphous phase decreases by a factor of e = 2.718, a_0 is a cell parameter of a growing crystal, Ω is the volume of the unit cell of a growing crystal. The difference in the determination of δ_0 is due to the fact, that in the case of LPC a single crystal (with a cell parameter a_0) is formed in the investigated region, and in the case of IPC (or DPC) a polycrystalline film (or dendrite), whose grains (or dendrite branches) have different orientations [19, 20].

The purpose of this work was to study the structure, morphology, and kinetics of electron-beam crystallization of amorphous films of hafnia and zirconia. Determining of the relative length δ_0 will make it possible to numerically classify the type of transformation. TEM with in situ video registration of structural evolution offers the possibility do it, since frame-by-frame analysis of the video allowed real-time measurement of the changes in number and size of the crystals, growing in amorphous film.

EXPERIMENTAL SECTION

The samples were free-standing amorphous films of hafnia and zirconia with a thickness $h \approx 30$ nm, obtained by pulsed laser evaporation. Laser erosion plasma was deposited on substrates of (001) KCl at room temperature. Sputtering of a high-purity Hf and Zr targets was carried out in an oxygen atmosphere ($P(O_2) \sim 0.13$ Pa) with the use of pulsed laser radiation from an LTI-PCh-5 laser operating in the Q-switched mode. The wavelength and the pulse repetition rate were equal to 1.06 μm and 25 Hz, respectively. Films were separated from the substrate in distilled water and transferred onto subject grids for electron microscopy studies.

Features of the a-c phase transformation were studied by electron diffraction and transmission electron microscopy (TEM) at the accelerating voltage of 100 kV. Crystallization was initiated by the electron beam impact inside the column of the electron microscope. This made it possible to register the structural transformations "in situ". The radiation dose rate was estimated from the beam current and the diameter of the electron beam focused at the sample. At a current of 20 μA and a diameter of 5 μm the radiation dose rate was ~ $6 \cdot 10^4$ $e^-/(Å^2 \cdot s)$.

Canon Power Shot G15 camera at the frame rate of 30 s^{-1} was used for video recording of the crystallization process. The captured film frames were used to construct crystallization kinetic curves $x=x(t)$. Electron microscopic visualization of crystals in an amorphous matrix was carried out in the bright field mode due to the different nature of the contrast of the amorphous (thickness contrast) and crystalline (diffraction contrast) phases. The crystals in the reflective position appeared dark against the gray background of the amorphous matrix. And the crystals not in a reflective position looked light against the gray background of the amorphous matrix. We measured the total area, occupied by the crystals at the electron microscope image of the analyzed space of the film. The content of the crystalline fraction x in the video frame we defined according to the ratio

$$x = \frac{S(t)}{S_f}, \tag{4}$$

where $S(t)$ is the area occupied by the crystalline phase in the frame at an arbitrary time moment t and S_f is the area of the field of the study. The crystal diameter $D(t)$ at a time t was determined according to the relation

$$D(t) = \sqrt{\frac{4S_k(t)}{\pi}}, \tag{5}$$

where $S_k(t)$ is the area of the crystal image at the time t. The average size of the crystals:

$$\langle D \rangle = \frac{1}{N}\sum_1^N D_i, \tag{6}$$

where D_i is the diameter of a single crystal, taken at number of i.

RESULTS AND DISCUSSION

Fig. 1,a and Fig. 2,a shows the electron diffraction (ED) patterns respectively from the free-standing film of hafnia and zirconia immediately after their separation from the substrate of KCl. They consist of two diffraction halos. The first halo is intense, while the second halo is much weaker in the intensity and very diffuse. According to the ED pattern, presented at Fig. 1,a and Fig. 2,a, the films are amorphous at the initial state. The action of the electron beam initiates in them growth of disoriented crystals, as evidenced by the ED patterns and electron microscope images, shown respectively at Fig. 1,b, c for hafnia and at Fig. 2,b, c for zirconia.

According to the electron diffraction pattern at Fig. 1,b, the crystalline phase of hafnia corresponds to monoclinic modification of HfO_2 [8]. In the amorphous film dendritic crystals are formed, consisting of

branches of the first, second and third order (see Fig. 1,c). Crystalline phase of zirconia corresponds to cubic modification of ZrO_2 [13], as evidenced by the electron diffraction pattern at Fig. 2,b. In contrast to HfO_2, crystals of ZrO_2 do not form dendrites, but have a predominantly equiaxed structure (see Fig. 2,c). The absence of reflections, associated with Hf and Zr, indicates on the one stage polymorphous character of the a-c transformation of hafnia and zirconia.

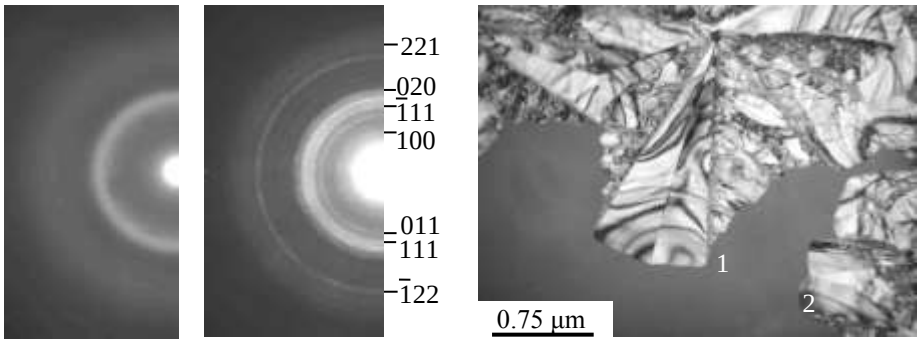

Fig. 1. Electron-beam crystallization of the amorphous HfO_2 film: ED patterns of the initial state (a) and after partial crystallization of the film (b); TEM image of the film after partial crystallization (c); 1 – amorphous phase; 2 – crystal phase

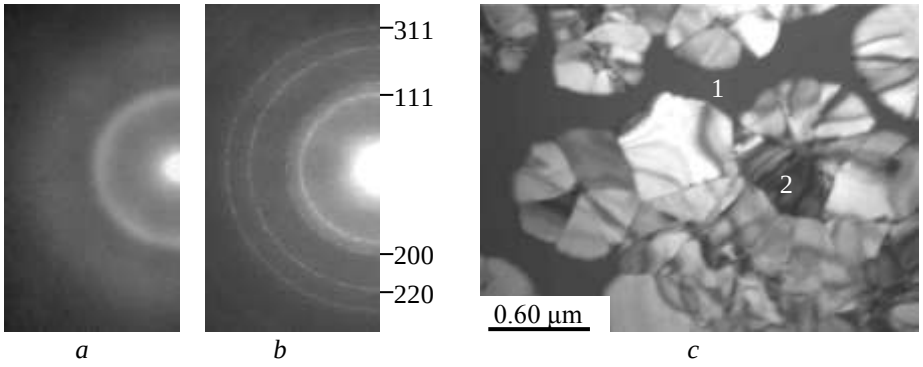

Fig. 2. Electron-beam crystallization of the amorphous ZrO_2 film: ED patterns of the initial state (a) and after partial crystallization of the film (b); TEM image of the film after partial crystallization (c); 1 – amorphous phase; 2 – crystal phase

Fig. 3 shows TEM video footage of dendrite growth in amorphous films of hafnia. Time moments *t* that has passed from the beginning of the recording of the crystallization process is shown in the upper right corner of each frame. A one-stage transformation is realized: amorphous phase – dendrite HfO_2 of a monoclinic modification. First-order dendritic branches are formed in the center of the cluster. Branches of the second order are formed mainly at the lateral surface of the branches of the first order.

Fig. 4 shows TEM video footage of crystals growth in amorphous films of zirconia. Time moments *t* that has passed from the beginning of the recording of the crystallization process is shown in the upper right corner of each frame. A one-stage transformation is realized: amorphous phase – crystal ZrO_2 of a cubic modification.

The kinetic curves of the dendrite growth are shown at Fig. 5,a. They correspond to the frames at Fig. 3. Line 1 shows the dependence on time of the dendritic intergrowth diameter *D*. Lines 2 and 3 shows the dependence on time of the length h_1 of the first order dendrite branch and of the length h_2 of the second order dendrite branches respectively. Lines 1, 2, and 3 correspond to the equations:

$$D = 1.350t + 0.043 \text{ μm}, \quad (7a)$$

$$h_1 = 1.215t + 0.051 \text{ μm}, \quad (7b)$$

$$h_2 = 0.744t - 0.029 \text{ μm}. \quad (7c)$$

According to (7) the increase of *D*, h_1 and h_2 occurs at a constant rate v_D = 1.350 μm·s^{-1}, v_1 = 1.215 μm·s^{-1} and v_3 = 0.744 μm·s^{-1} respectively. The ratio $v_1 > v_2$ shows, that the dendrite branches of the first order grow faster than the dendrite branches of the second order. The later the branch appeared, the more slowly it grows.

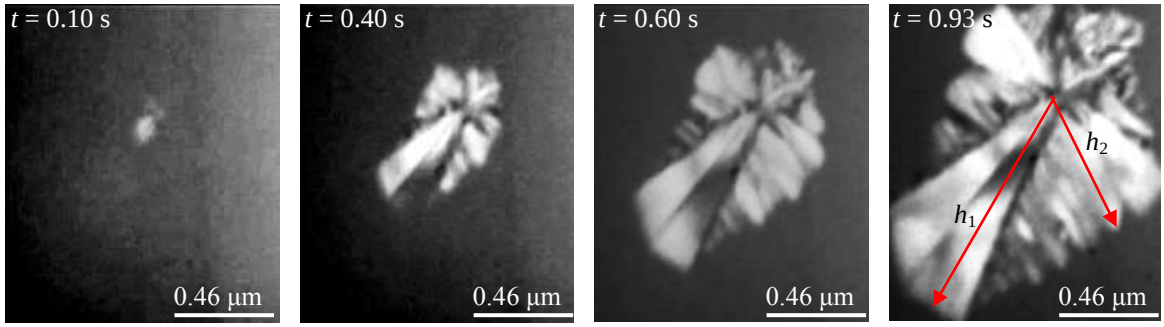

Fig. 3. TEM video footage of dendrite growth in amorphous films of hafnia. Time moments t, that has passed from the beginning of the recording of the crystallization process, are shown in the upper right corner of each frame. h_1 is the length of the first order branch; h_2 is the length of the second-order branch

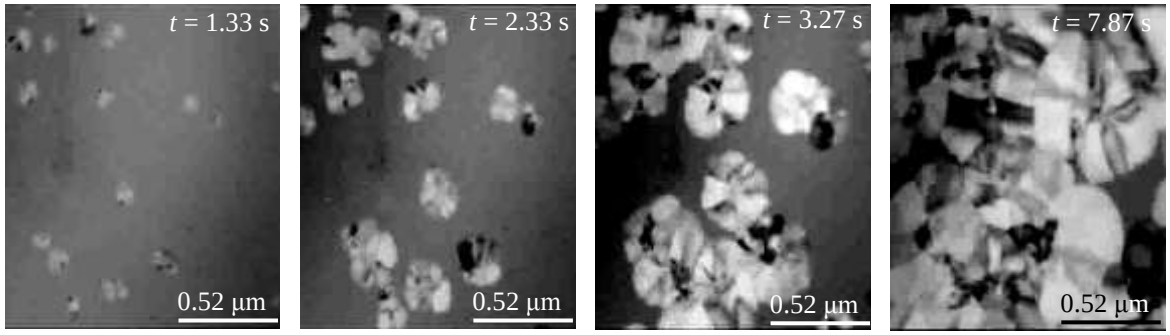

Fig. 4. TEM video footage of crystals growth in amorphous films of zirconia. Time moments t, that has passed from the beginning of the recording of the crystallization process, are shown in the upper right corner of each frame

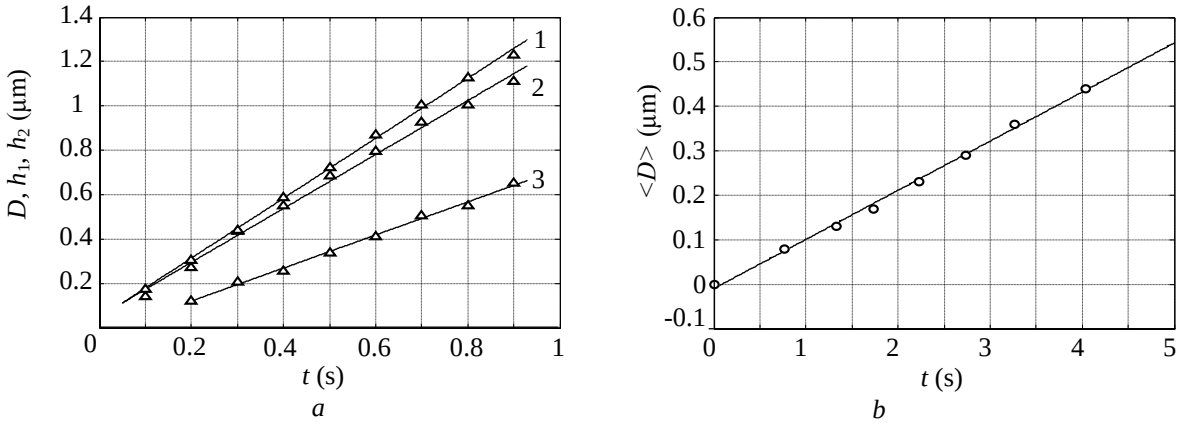

Fig. 5. The kinetic curves of the dendrite growth in amorphous film of HfO_2. Line 1 shows the dependence on time of the dendritic diameter D. Lines 2 and 3 shows the dependence on time of the length h_1 of the first order and h_2 of the second order dendrite branches respectively (a). The dependence on time of the average diameter <D> of crystals, growing in amorphous film of ZrO_2 (b)

Fig. 5,b shows the dependence on time of the average diameter <*D*> of crystals, growing in amorphous film of ZrO_2. This line corresponds to the equation:

$$<D> = 0.110t - 0.010 \text{ μm}. \quad (8)$$

According to (8) the increase of <*D*> occurs at a constant rate $v_{<D>} = 0.110$ μm·s^{-1}.

Time dependence of the crystallized volume fraction *x*(*t*) of hafnia is shown at Fig. 6,a. This experimental data, presented in the coordinates $x - t^2$, form a straight line (see Fig. 6,b). This fact indicates a quadratic dependence *x*(*t*):

$$x = 0.799\, t^2 + 0.015. \quad (9)$$

Time dependence of the crystallized volume fraction *x*(*t*) of zirconia is shown at Fig. 7,a. This experimental data, presented in the coordinates ln[-ln(1-*x*)] - ln*t*, form a straight line (see Fig. 7,b). This fact indicates the applicability to the process of a-c phase transformation of the JMAK formulas (1). Drawing ln[-ln(1-x)] against ln(*t*) should be straight line:

$$\ln[-\ln(1-x)] = n\ln t + \ln k. \quad (10)$$

In this case *n* is the tangent of the angle of inclination of the line to the abscissa and the point of the intersection with the ordinate is ln*k*. According to (10) and Fig. 7,b $n = 2.03$, $\ln k = -2.976$, and $k = 0.051$ s^{-2}. Taking into account numerical values of *n* and *k*, the curve at Fig. 7,a will fit the equation:

$$x = 1-\exp(-0.051t^{2.03}). \quad (11)$$

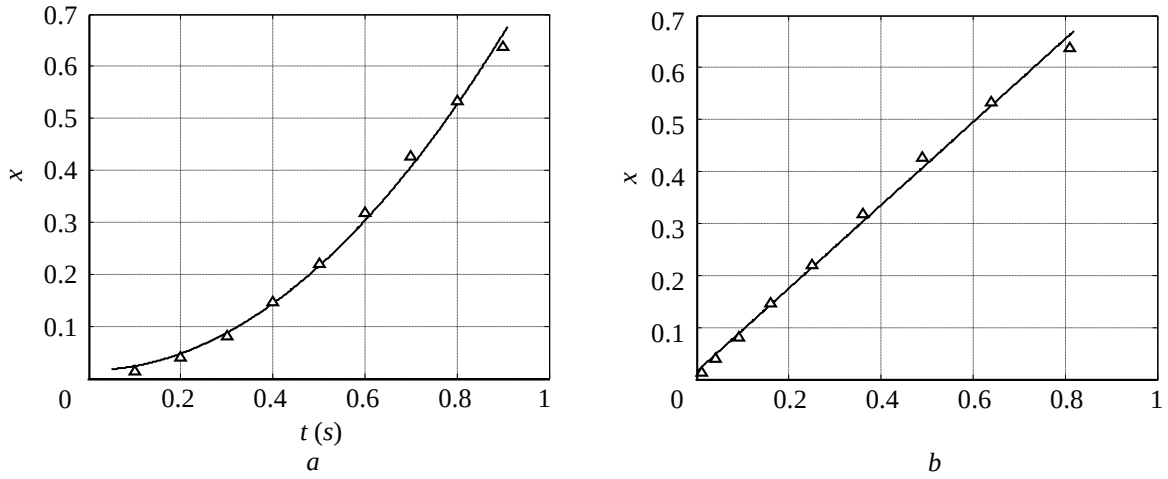

Fig. 6. The dependence on time of the crystallized volume fraction x(t) of amorphous HfO_2 film in coordinates x - t (a) and in coordinates x - t^2 (b)

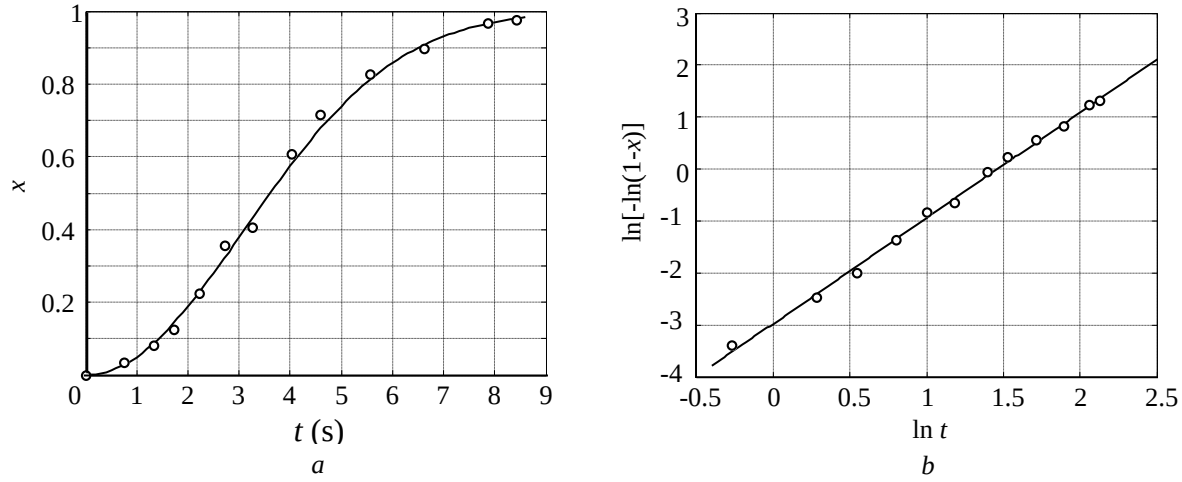

Fig. 7. The dependence on time of the crystallized volume fraction x(t) of amorphous ZrO_2 film in coordinates x - t (a) and in coordinates ln[-ln(1-x)] - lnt (b)

CONCLUSIONS

Amorphous films of hafnia and zirconia are formed on substrates at room temperature in the process of pulsed laser evaporation of Hf and Zr targets in an oxygen atmosphere. Irradiation of amorphous film with the electron beam initiates its crystallization. The transformation has one-stage character. The amorphous hafnia polymorphically passes into the crystalline one with monoclinic modification of HfO_2. According to the video recording data (see Fig. 3) during crystallization of the film a single dendrite grows in the field of observation. The dendrite grows at the constant rate at the constant intensity of electron beam irradiation of the film. In this case D, h_1, and $h_2 \sim t$. The crystalline fraction $x \sim t^2$. These structural and morphological characteristics qualitatively indicate the implementation of the DPC mode.

The amorphous zirconia polymorphically passes into the crystalline one with cubic modification of ZrO_2. According to the video recording data (see Fig. 4) during crystallization of the film multiple crystals grows in the field of observation. Nucleation happens only at the beginning and growth takes place afterwards. Each crystal grows at the constant rate at the constant intensity of electron beam irradiation of the film. This nucleation mechanism would be identified as a Site-Saturate Nucleation (SSN) [14]. In this case $\langle D \rangle \sim t$ and $x(t) = 1\text{-}\exp(-kt^n)$. The Avrami exponent $n = 2.03$ (nearest integer = 2). It contains information about growth dimensionality (N). For site-saturated nucleation $n = N$. These structural and morphological characteristics qualitatively indicate the implementation of the IPC mode.

The value of the relative crystallization length δ_0 provides quantitative information about which crystallization mode is realized. In the case of HfO_2 when the fraction of the crystalline phase $x = 0.632$, according to (9) and Fig 6,a the characteristic unit of time $t_0 = 0.879$ s. According to (7a) the characteristic unit of the length $D_0 \approx 1.230$ μm. For HfO_2 the volume of unit cell $\Omega = 1.3828 \cdot 10^{-10}$ μm^3 [8]. In this case, according to (3), the relative length $\delta_0 \approx 2380$ (several thousand is a number, typical for DPC mode [17]).

In the case of ZrO_2 when the fraction of the crystalline phase $x = 0.632$, according to (11) and Fig. 7,a the characteristic unit of time $t_0 = 4.331$ s. In agreement with (8) the characteristic unit of the length $D_0 \approx 0.466$ μm. For ZrO_2 the volume of unit cell

$\Omega = 1.3187 \cdot 10^{-10}$ μm^3 [13]. In this case, according to (3), the relative length $\delta_0 \approx 915$ (several hundred is a numeric, typical for IPC mode [17]).

REFERENCES

1. W.T. Tang, Z.F. Ying, Z.G. Hu, W.W. Li, J. Sun, N. Xu, J.D. Wu. Synthesis and characterization of HfO_2 and ZrO_2 thin films deposited by plasma assisted reactive pulsed laser deposition at low temperature // *Thin Solid Films*. 2010, v. 518, p. 5442-5446; https://doi.org/10.1016/j.tsf.2010.04.012
2. D. Hausmann, R. Gordon. Surface morphology and crystallinity control in the atomic layer deposition (ALD) of hafnium and zirconium oxide thin films // *J. Cryst. Growth*. 2003, v. 249, p. 251-261; https://doi.org/10.1016/S0022-0248(02)02133
3. L. Zhang, J. Zhang, H. Jiao, G. Bao, Z. Wang, X. Cheng. Thickness-dependent surface morphology and crystallization of HfO_2 coatings prepared with ion-assisted deposition // *Thin Solid Films*. 2017, v. 642, p. 359-363; https://doi.org/10.1016/j.tsf.2017.10.010
4. D. Vanderbilt, X. Zhao, D. Ceresoli. Structural and dielectric properties of crystalline and amorphous ZrO_2 // *Thin Solid Films.* 2005, v. 486, p. 125-128; https://doi.org/10.1016/j.tsf.2004.11.232
5. R. Tokas, S. Jena, J. Misal, K. Rao, S. Polaki, C. Pratap, D. Udupa, S. Thakur, S. Kumar, N. Sahoo. Study of ZrO_2 thin films deposited at glancing angle by radio frequency magnetron sputtering under varying substrate rotation // *Thin Solid Films*. 2018, v. 645, p. 290-299; https://doi.org/10.1016/j.tsf.2017.11.007
6. S. Kim, Y. Oshima, N. Nakajima, N. Hashikawa, K. Asayama, K. Takayanagi. Direct observation of crystallization of HfO_2 promoted on silicon surfaces in gate dielectric stacks // *Thin Solid Films*. 2012, v. 520, p. 2562-2565 2012; https://doi.org/10.1016/j.tsf.2011.11.001
7. L.W. Hobbs. *Radiation effects in analysis of inorganic specimens by TEM* / J.J. Hren, J.I. Goldstein, D.C. Joy (Eds.). Introduction to Analytical Electron Microscopy, Plenum, New York, 1979, p. 437-490; https://link.springer.com/chapter/10.1007/978-1-4757-5581-7_17
8. *Powder Diffraction File.* Joint Committee on Powder Diffraction Standards, International Center for Diffraction Data, Swarthmore, Philadelphia, United States, 1996, Card No. 43-1017.
9. *Powder Diffraction File.* Joint Committee on Powder Diffraction Standards, International Center for Diffraction Data, Swarthmore, Philadelphia, United States, 1996, Card No. 08-0342.
10. *Powder Diffraction File.* Joint Committee on Powder Diffraction Standards, International Center for Diffraction Data, Swarthmore, Philadelphia, United States, 1996, Card No. 21-0904.
11. *Powder Diffraction File.* Joint Committee on Powder Diffraction Standards, International Center for Diffraction Data, Swarthmore, Philadelphia, United States, 1996, Card No. 37-1484.
12. *Powder Diffraction File.* Joint Committee on Powder Diffraction Standards, International Center for Diffraction Data, Swarthmore, Philadelphia, United States, 1996, Card No. 17-0923.
13. *Powder Diffraction File.* Joint Committee on Powder Diffraction Standards, International Center for Diffraction Data, Swarthmore, Philadelphia, United States, 1996, Card No. 27-0997.
14. M. Moghadam, P. Voorhees. Thin film phase transformation kinetics: from theory to experiment // *Scripta Materialia*. 2016, v. 124, p. 164-168; https://doi.org/10.1016/j.scriptamat.2016.07.010
15. A. Shirinyan, Yu. Bilogorodskyy. Effect of radiation-induced vacancy saturation on the first-order phase transformation in nanoparticles: insights from a model // *Beilstein J. Nanotechnol.* 2024, v. 15, p. 1453-1472; https://doi.org/10.3762/bjnano.15.117
16. N. Ohshima. Crystallization of germanium–antimony–tellurium amorphous thin film sandwiched between various dielectric protective films // *J. Appl. Phys.* 1996, v. 79, p. 8357-8363; https://doi.org/10.1063/1.362548
17. A. Bagmut. Layer, island and dendrite crystallizations of amorphous films as analogs of Frank–van der Merwe, Volmer–Weber and Stranski–Krastanov growth modes // *Func. Mater*. 2019, v. 26, p. 6-15; https://doi.org/10.15407/fm26.01.6
18. A. Bagmut. Relative length as a classification parameter of the crystallization mode of amorphous films // *Problems of Atomic Science and Technology.* 2022, N 1(137), p. 64-68; https://doi.org/10.46813/2022-137-064
19. A. Bagmut, I. Bagmut, A. Devizenko. In situ TEM study of crystals growth in amorphous Ti-Zr-Ni films at electron beam irradiation // *Eur. Phys. J. Appl. Phys*. 2023, v. 98, p. 1-8; https://doi.org/10.1051/epjap/2023220293
20. A. Bagmut. Crystal growth in amorphous films of tantalum pentoxide // *Molecular Crystals and Liquid Crystals.* 2023, v. 765, p. 105-113; https://doi.org/10.1080/15421406.2023.2215032W

Article received 18.06.2024

РАДІАЦІЙНО ПОСИЛЕНА КРИСТАЛІЗАЦІЯ АМОРФНИХ ЛАЗЕРНИХ КОНДЕНСАТІВ ГАФНІЮ І ЦИРКОНІЮ

О.Г. Багмут

Досліджено кристалізацію аморфних плівок гафнію (HfO_2) та цирконію (ZrO_2) під дією електронного опромінення. Електронно-мікроскопічні дослідження «in situ» з відеореєстрацією структурних змін показали, що фазове перетворення у гафнії відбувається за дендритною поліморфною модою кристалізації з відносною довжиною $\delta_0 \approx 2380$, а у цирконії – за острівцевою поліморфною модою кристалізації з відносною довжиною $\delta_0 \approx 915$. Залежність частки кристалічної фази від часу для гафнію має квадратичний характер, а для цирконію – експоненціальний, що описується формулою Johnson-Mehl-Avrami-Kolmogorov (JMAK).